A New *N*-Channel Maximum Entropy Method in NMR for Automatic Reconstruction of "Decoupled Spectra" and *J*-Coupling Determination

V. Stoven,*,† J. P. Annereau,† M. A. Delsuc,‡ and J. Y. Lallemand†

Laboratoire de RMN, DCSO, Ecole Polytechnique, 91190 Palsaiseau Cedex, France, and Centre de Biochimie Structurale, Faculté de Pharmacie, 15 avenue Charles Flahault, 34000 Montpellier, France

Received April 12, 1996⊗

A new *N*-channel (or multichannel) deconvolution method of 1D and 2D NMR spectra is presented based on the Maximum Entropy method. In the general case of spectra exhibiting several lines of various fine structures, the method allows simultaneous deconvolution of all lines. While deconvolution is performed, determination of the values of the coupling constants is possible. Reconstruction of "decoupled" 1D and 2D spectra is also performed in a fully automated approach. The efficiency of the method is illustrated on experimental 1D and 2D spectra. The method has been developed in the GIFA software, a complete package for processing of NMR data available from the authors.

INTRODUCTION

The NMR signal in 1D and 2D spectra contains three types of valuable information for structural analysis of molecules: frequency (or chemical shift), amplitude, and wide-sense line shape (including both line width and *J* coupling modulation). The latter often results in complex multiplet patterns, leading to altered resolution and signal-to-noise ratio (S/N). Since only chemical shift information is needed for spectral assignment, whereas *J* coupling information is only needed for conformational analysis,[1] separation of chemical shift and line shape information is of great practical interest. The idea developed in this work is to collapse multiplets into singlets of increased intensity, providing a "decoupled" spectrum to simplify the assignment procedure and keeping the *J* values for a separate use, as illustrated in Figure 1. This precisely illustrates the concept of deconvolution in NMR.

Since the pioneering work of Ernst,[2] many valiant efforts have been made to obtain "decoupled" spectra. Two approaches can be distinguished: deconvolution methods (self-deconvolution of multiplets,[3] convolution by the reciprocal of the convolution function,[4] *J* doubling,[5,6] MaxEnt[7,8]), and nonlinear methods based on local symmetry analysis.[9−11] However, we would stress that, in order to be used in everyday practice, a "decoupling" method should (i) be implemented in both 1D and 2D NMR, (ii) handle simultaneous deconvolution of many multiplets of various fine structures (i.e., perform *N*-channel *J* deconvolution), and (iii) be fully automatic. In this paper, we present a new deconvolution method based on the Maximum Entropy method (MaxEnt) that satisfies all the above criteria. This new development is the first one that allows simultaneous deconvolution of 1D and 2D spectra exhibiting several multiplets with various fine structures. Reconstruction of deconvoluted spectra is achieved using a fully automated procedure.

In the following, the concepts of convolution and the classical monochannel MaxEnt approach are first recalled. Next, the new generalized 1D and 2D *N*-channel deconvolution approach is presented. The method has been extensively tested on simulated data, but its efficiency will be demonstrated on experimental 1D and 2D NMR data.

THE CONCEPT OF CONVOLUTION AND DECONVOLUTION

The NMR Free Induction Decay (FID) of a system containing *N* spins, each spin having a particular line shape, is a time function that can be expressed as

$$s(t) = \sum_{k=1}^{N} i_k(t) \times c_k(t) + n(t) \qquad (1)$$

where i_k bears the chemical shift information, c_k bears the line width and complete *J* pattern information, and *n* is the noise function. Equation 1 has the equivalent expression for the frequency spectrum, by Fourier transformation (FT)

$$S(\omega) = \sum_{k=1}^{N} I_k(\omega) * C_k(\omega) + N(\omega) \qquad (2)$$

where * represents a convolution product, and I_k, C_k, and N are the FT of i_k, c_k, and n, respectively. In the approximation of weak coupling, in the case of Lorentzian lineshapes, function c_k of spin k is expressed in the time domain as

$$c_k(t) = \prod_{i,j} \sin(\pi J_k^i t) \times \cos(\pi J_k^j t) \times \exp(-t/\tau_k) \qquad (3)$$

where J_k^j and J_k^i represent, respectively, all the active and passive couplings applied to spin k. c_k is called the convolution function, and τ_k is the damping factor. However, the damping term will be ignored in the following, for sake of simplicity. Then, in the frequency domain, eq 3 becomes

$$C_k(\omega) = \prod_{i,j} A_k^i(J_k^i,\omega) * P_k^j(J_k^j,\omega) \qquad (4)$$

where $P_k^j(J_k^j,\omega)$ and $A_k^i(J_k^i,\omega)$ are, respectively, in-phase and anti-phase doublets, which determine the fine structure of the peak associated to spin k.

* Corresponding author.
† Ecole Polytechnique.
‡ Centre de Biochimie Structurale.
⊗ Abstract published in *Advance ACS Abstracts,* October 1, 1996.

S0095-2338(96)00321-6 CCC: $14.00

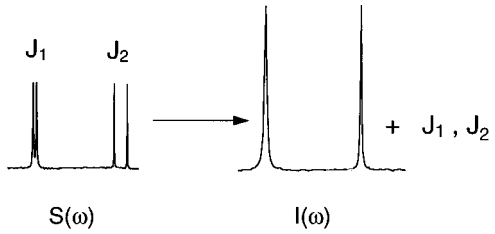

Figure 1. 1D spectrum displaying two lines with in-phase couplings. A deconvolution method should restore singlets of double intensity, i.e., separation of chemical shift and coupling constant information.

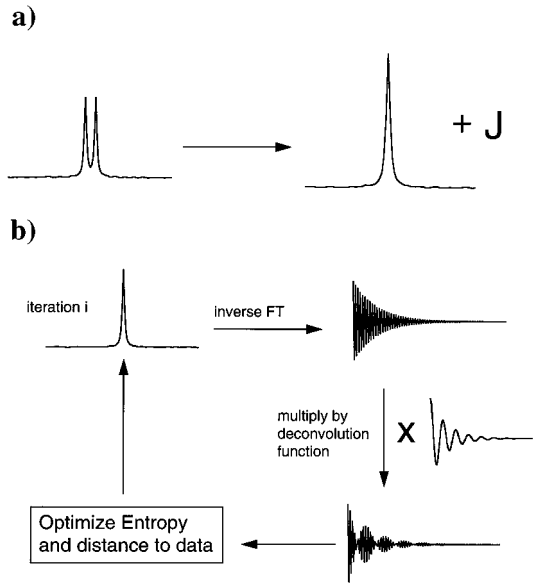

Figure 2. (a) Mono channel deconvolution methods can process one line or several lines if they have identical line shapes. (b) Principle of monochannel MaxEnt deconvolution. The spectrum shown in Figure 2a is processed. At each iteration, the MaxEnt FID is calculated by inverse FT of the current MaxEnt spectrum. This pseudo FID is multiplied by the deconvolution function (cos(πJt) function here). Optimization of Entropy and distance to data is performed before computing the next MaxEnt spectrum.

Deconvolution of $S(\omega)$ consists in the reconstruction of a fully decoupled $I(\omega)$ spectrum defined by

$$I(\omega) = \sum_{k=1}^{N} I_k(\omega) \tag{5}$$

$I(\omega)$ contains shear frequency information devoid of line shape information, as illustrated in Figure 1.

Since each spin is associated to a particular convolution function, two strategies can be adopted.

The first one is to use a classical mono channel deconvolution method. Each multiplet is extracted from the original spectrum and processed separately (Figure 2a). Then the fully deconvoluted spectrum can eventually be reconstructed. This is the most widely chosen option, although it implies a quite tedious process and cannot be easily automated.

The second strategy is to use a generalized *N*-channel deconvolution method. This is a more efficient approach. Here, no prior extraction of multiplets is necessary, and a unique *N*-channel process achieves simultaneous deconvolution of all multiplets. Unfortunately, all methods are not suitable for such *N*-channel generalization: direct methods will usually not present the required computational stability. This problem can be avoided by inverse reconstruction methods using the MaxEnt strategy. Indeed, it will be shown that MaxEnt can be extended to *N*-channel deconvolution of 1D and 2D spectra.

A BRIEF ACCOUNT ON CLASSICAL DECONVOLUTION BY MAXIMUM ENTROPY

Detailed description of MaxEnt is beyond the scope of this paper and will not be presented. Its applications in NMR have already been discussed,[12] and many authors have successfully applied this inverse method to reconstruct multidimensional NMR spectra.[12−14] However, for sake of clarity, before presenting the new *N*-channel algorithm, we will briefly recall the bases of classical MaxEnt reconstruction of NMR spectra, which allows monochannel deconvolution.

The experimental NMR (FID) $s(t)$ is a time domain function related to its spectrum $S(\omega)$ by Fourier Transformation. Similarly, MaxEnt provides another strategy. The MaxEnt reconstructed spectrum $S'(\omega)$ is related through a transform T, to a pseudo FID (or MaxEnt FID) $s'(t)$, the latter being an as good as possible approximation of the experimental data $s(t)$. This condition is achieved when the distance D between the pseudo and experimental spectra is of the order of the noise. D is defined by

$$D = \chi^2 = \int (s(t) - s'(t))^2 \, dt/\sigma^2$$

with

$$s'(t) = T(S'(\omega)) \tag{6}$$

where σ is the mean standard noise deviation of the recorded FID $s(t)$. In practice, $s(t)$ is a discrete function of M points, and D reaches its optimum when $D = M$. In the simplest case (no deconvolution), T equals the inverse FT

$$T(S'(\omega)) = s'(t) = FT^{-1}(S'(\omega)) \tag{7}$$

Unfortunately, because the FID signal is finite and noisy, many $S'(\omega)$ spectra fulfill the condition that D is optimum. However, we know from the information theory that, among all the trial spectra that satisfy eq 6, one must choose the spectrum the entropy of which is maximum.[15,16] This spectrum equivalently contains the minimum information. The entropy of $S'(\omega)$ is defined as

$$E = -\int S'(\omega) \times \log(S'(\omega)/A) \, d\omega \tag{8}$$

where A is a normalization constant:

$$A = \int S'(\omega) \, d\omega \tag{9}$$

Hence, the MaxEnt spectrum should simultaneously satisfy two criteria: (i) D is minimum (χ^2 = M) and (ii) E is maximum. This condition is fulfilled by maximizing the function Q defined by

$$Q = E - \lambda D \tag{10}$$

where λ is a Lagrange multiplier. The algorithm that we developed to perform this maximization is the GIFA algorithm.[17] GIFA is derived from the Gull and Daniell algorithm.[18] Its efficiency in reconstruction of 1D or 2D NMR spectra has already been proven.[14]

Let us show now that MaxEnt also enables deconvolution of a spectrum. If the spin system is composed of *N* spins

with identical convolution function (i.e., identical fine structures), the expression of the FID (eq 1) becomes

$$s(t) = c(t) \times \sum_{k=1}^{N} i_k(t) + n(t) \tag{11}$$

If $c(t)$ is known, this prior knowledge can be introduced in T, which adopts a new expression, defining a new deconvoluted MaxEnt spectrum $I'(\omega)$

$$T(I'(\omega)) = s'(t) = c(t) \times FT^{-1}(I'(\omega)) \tag{12}$$

In this case, the entropy and normalization constants are calculated on $I'(\omega)$, and distance D is evaluated between a "reconvoluted" $s'(t)$ pseudo FID and the data $s(t)$. A scheme of the algorithm is presented in Figure 2b.

As mentioned above, the monochannel approach applies only to situations where all spins have a common convolution function. Obviously, this is usually not the case. In the next section, we present a new *N*-channel generalization that can handle situations where different convolution functions are present.

PRINCIPLE OF *N-CHANNEL* MAXENT DECONVOLUTION IN 1D AND 2D NMR

The experimental FID adopts now the more general expression

$$s(t) = \sum_{k=1}^{N} i_k(t) \times c_k(t) + n(t) \tag{13}$$

The idea underlying *N*-channel deconvolution is to simultaneously build *N* subspectra $I'(\omega,k)$ (or *N* channels associated to the c_k convolution functions), each of which displaying a unique and singlet peak at the frequency of spin k. This set of spectra form a *N*-channel deconvoluted MaxEnt spectrum, which can be viewed as a 2D spectrum, the dimension of which is higher than that of the data. This new dimension bears the spin numbers (or the convolution type numbers, when several spins have the same convolution function). Therefore, a new T transform needs to be applied to $I'(\omega,k)$. T and $s'(t)$ are defined as

$$T(I'(\omega,k)) = s'(t) = \sum_{k=1}^{N} c_k(t) \times FT^{-1}(I'(\omega,k)) \tag{14}$$

T can be understood as a projection along the k axis to be applied on *N* MaxEnt FIDs, so that comparison to the experimental data is possible. χ^2 can now be evaluated between the projection $s'(t)$ and the data $s(t)$ according to eq 6. The entropy is however evaluated on the whole MaxEnt spectrum $I'(\omega,k)$ with the expression

$$S = \sum_{k=1}^{M} \int I'(\omega,k) \log(I'(\omega,k)/A)\, \mathrm{d}\omega \tag{15}$$

A scheme of the algorithm is presented in Figure 3. When convergence is reached, each line exhibits significant intensity only in the channel corresponding to its own convolution function. In the GIFA program, a fully deconvoluted spectrum having the same dimension that the data are further recovered after automatic peak detection in the different channels.[19]

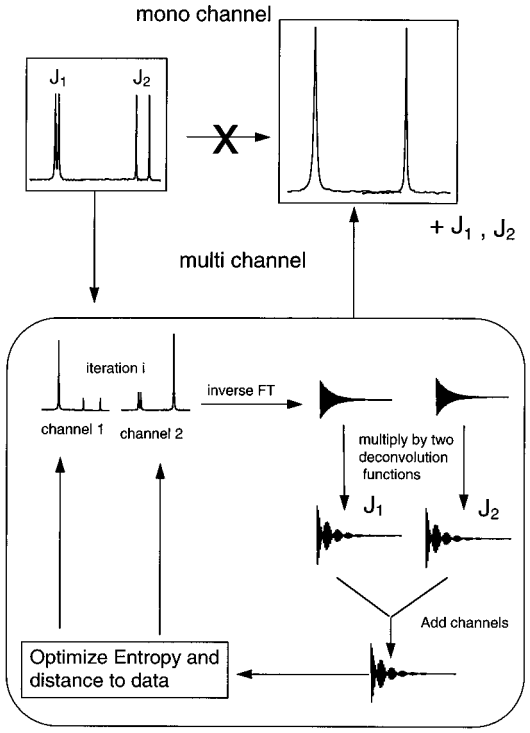

Figure 3. Monochannel methods cannot process spectra containing several lines of various fine structures in a single step. The scheme of the new *N*-channel MaxEnt algorithm is shown, in the case of a 1D spectrum. Two deconvolution channels are used because two line shapes are present in the spectrum. The associated deconvolution functions are $\cos(\pi J_1 t)$ and $\cos(\pi J_2 t)$. Addition of the two channels is necessary before the optimization step. When convergence is reached, each line presents maximum intensity in the channel bearing its own convolution function. Automatic peak picking in the two channels enables recovery of a 1D deconvoluted spectrum.

Although the method has been presented above in the case of 1D NMR spectra, we have generalized the algorithm for 2D NMR spectra. Similarly, an additional variable is introduced to define a 3D MaxEnt spectrum $I'(\omega_1,\omega_2,k)$. Transform T takes again the form of a projection along the new axis, to compute a 2D MaxEnt FID $s'(t_1,t_2)$

$$T(I'(\omega_1,\omega_2,k)) = s'(t_1,t_2) = \sum_{k=1}^{N} c_k(t_1,t_2) \times FT_{1,2}{}^{-1}(I'(\omega_1,\omega_2,k)) \tag{16}$$

Then, χ^2 can be evaluated as usual between $s'(t_1,t_2)$ and the experimental data $s(t_1,t_2)$. The entropy is however evaluated on the whole 3D MaxEnt spectrum.

$$S = \sum_{k=1}^{N} \int\int I'(\omega_1,\omega_2,k) \log(I'(\omega_1,\omega_2,k)/A)\, \mathrm{d}\omega_1\, \mathrm{d}\omega_2 \tag{17}$$

This generalization offers treatment of 2D data by a genuine 2D and *N*-channel algorithm: a 2D MaxEnt FID $s'(t_1,t_2)$ is generated when the data is a set of 2D FIDs $s(t_1,t_2)$. As in the 1D case, recovery of a fully deconvoluted (or "decoupled") 2D map is finally obtained after automatic 2D peak detection in the different channels.[19]

In conclusion of this section, it is important to understand that deconvolution of a 2D map by a 1D *N*-channel algorithm applied successively on all rows and columns may be possible in principle. However, this would require a cumbersome and time consuming process. Automation of

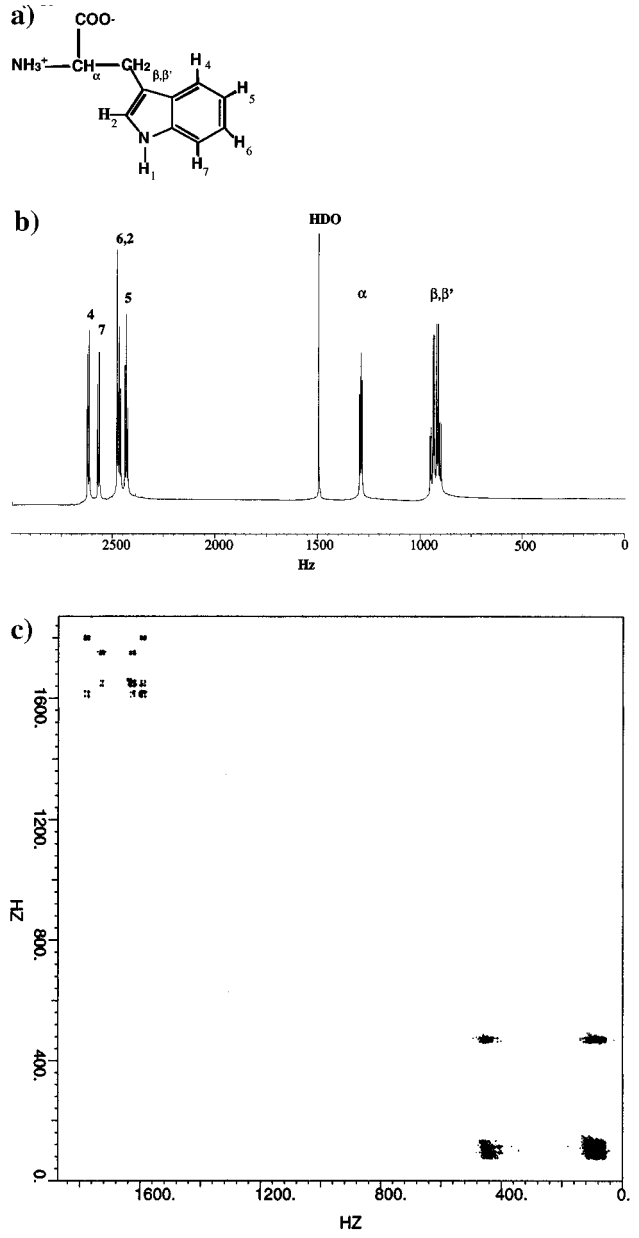

Figure 4. (a) Tryptophan molecule. Hydrogen atoms are labeled using conventional notations. (b) 1D spectrum of tryptophan, in D_2O at 303 K. Assignment of the spectrum is given. The central line arises from the solvent signal. Recording conditions: 16 scans of 16K data points each, spectral width of 2994 Hz. (c) 2D DQF-COSY of tryptophan, in D_2O at 303 K. Recording conditions: 1024 FIDs of 2048 data points each.

deconvolution and reconstruction of the 2D map using such an approach would be very difficult.

EXPERIMENTAL RESULTS

An illustration of this new method will be shown on 1D and 2D spectra of tryptophan. The tryptophan molecule is shown in Figure 4a. Its assigned 1D ^{1}H NMR spectrum in D_2O is shown in Figure 4b. Two regions can be distinguished: the aromatic region (left of the spectrum) and the aliphatic region (right of the spectrum). The 2D DQF-COSY spectrum in D_2O is shown in Figure 4c. Examples of *N*-channel deconvolution will be given in 1D NMR on the aliphatic region of the 1D ^{1}H spectrum and in 2D NMR on the aromatic region of the 2D DQF-COSY map.

1D Example. The aliphatic spin system is formed by protons α, β, and β'. A zoom in their ^{1}H NMR spectrum is presented in Figure 5a. The values of coupling constants existing in this spin system are accessible by first order analysis of the spectrum (with a digital resolution of 2994/16K Hz/pt):

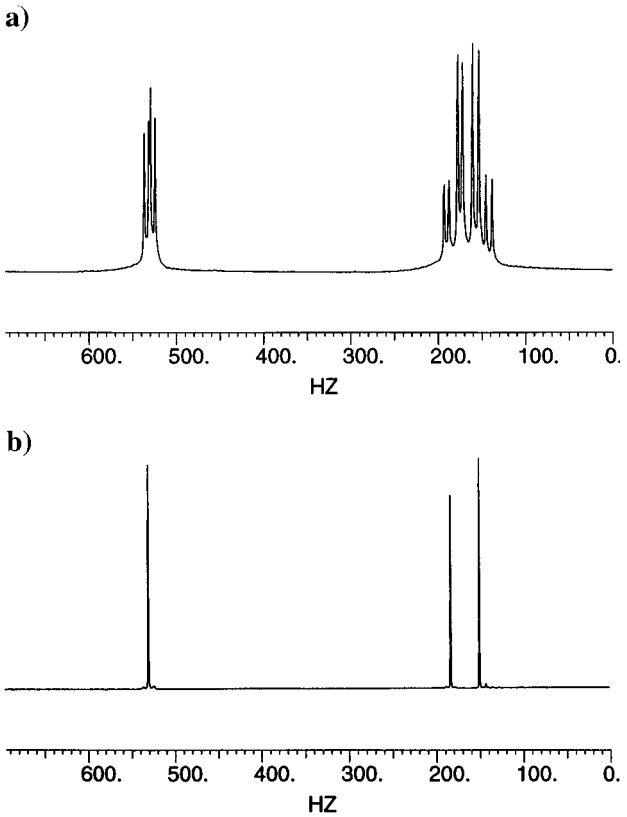

Figure 5. (a) Zoom in the aliphatic region of the 1D spectrum presented in Figure 4b. (b) Reconstruction of the spectrum presented in Figure 5a, after *N*-channel deconvolution. Convergence was obtained after 10 iterations.

$$J(\alpha,\beta) = 5.5 \text{ Hz}$$
$$J(\alpha,\beta') = 7.0 \text{ Hz} \quad (18)$$
$$J(\beta,\beta') = 15.0 \text{ Hz}$$

They all lead to in-phase couplings in this 1D spectrum. Thus, the convolution functions associated to protons α, β, and β' are

$$c_\alpha(t) = \cos(5.5\pi t) \times \cos(7\pi t)$$
$$c_\beta(t) = \cos(5.5\pi t) \times \cos(15\pi t) \quad (19)$$
$$c_{\beta'}(t) = \cos(7\pi t) \times \cos(15\pi t)$$

These three functions were introduced in three MaxEnt channels. When convergence was reached, deconvoluted peak indeed presented strong intensity only in the channel bearing its own convolution function. The reconstructed "decoupled" 1D spectrum is shown in Figure 5b. It is interesting to note that, despite a strong AB effect observed between protons β and β', the program did operate successfully.

2D Example. The aromatic spin system of tryptophan in D_2O is composed of protons 2, 4, 5, 6, and 7 (the N−H proton is exchanged). A zoom in the aromatic region of the 2D DQF-COSY spectrum is presented in Figure 6a. Proton 2 does not give a detectable signal in this 2D map, because it is not involved in any scalar coupling. First order

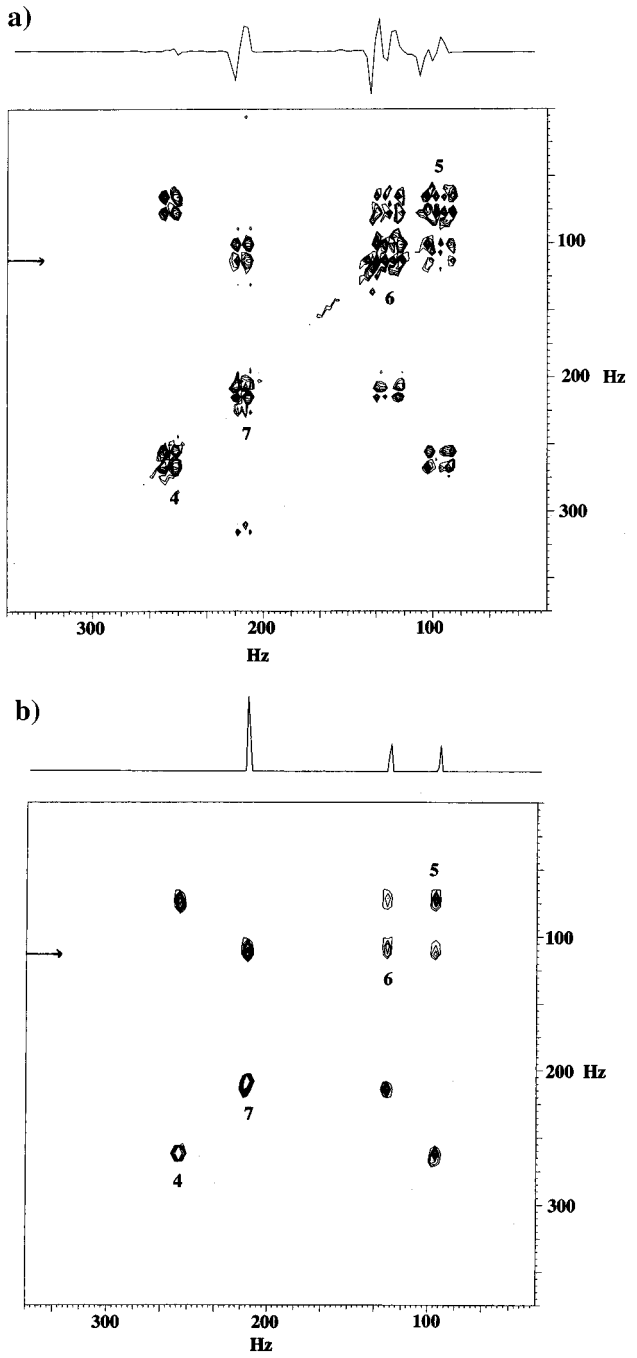

Figure 6. (a) Zoom in the aromatic region of the DQF-COSY presented in Figure 4c. A cross section is shown, taken at the frequency of proton 6 (indicated by the arrow). (b) Reconstruction of the spectrum presented in Figure 6a, after 2D *N*-channel deconvolution. Convergence was obtained after 12 iterations. A cross section is shown, taken at the frequency of proton 6 (indicated by the arrow).

analysis of the 1D spectrum showed that all coupling constants existing between protons 4, 5, 6, and 7 were equal to 8.2 Hz. Protons 4 and 7 present only one coupling constant

$$\begin{aligned} J(4,5) &= 8.2 \text{ Hz} \\ J(7,6) &= 8.2 \text{ Hz} \end{aligned} \tag{20}$$

whereas protons 5 and 6 present two coupling constants

$$\begin{aligned} J(4,5) = J(6.5) &= 8.2 \text{ Hz} \\ J(7,6) = J(6,5) &= 8.2 \text{ Hz} \end{aligned} \tag{21}$$

Therefore, both active and passive couplings appear in the DQF-COSY spectrum. Thus, four types of convolution functions are encountered in this spectrum. They were introduced in four channels

$$\begin{aligned} c_1(t) &= \sin(\pi J t_1) \times \sin(\pi J t_2) \\ c_2(t) &= \sin(\pi J t_1) \times \cos(\pi J t_1) \times \sin(\pi J t_2) \\ c_3(t) &= \sin(\pi J t_1) \times \sin(\pi J t_2) \times \cos(\pi J t_2) \\ c_4(t) &= \sin(\pi J t_1) \times \cos(\pi J t_1) \times \sin(\pi J t_2) \times \cos(\pi J t_2) \end{aligned} \tag{22}$$

where $J = 8.2$ Hz. The diagonal peaks of protons 4 and 7 should be found in channel 1. Those of protons 5 and 6 and off diagonal peaks correlating these two protons together should be found in channel 4. Off diagonal peaks of protons 4 and 7 should be found in channel 2 (above the diagonal) and 3 (under the diagonal). After 2D *N*-channel deconvolution, these peaks were indeed found in these predicted channels. The "decoupled" 2D spectrum reconstructed after deconvolution, is shown in Figure 6b.

These results demonstrate that the MaxEnt method can be generalized to *N*-channel deconvolution in 1D and 2D NMR. Simplified spectra are obtained, with the benefit of increased resolution and S/N, as examplified by two cross sections in Figure 6a,b. The above examples were used to test the feasability of this approach, since prior knowledge of all coupling constants and convolution functions was assumed. In the next section, we will show how to apply this method in more general cases where the complete *J* pattern is not known beforehand. In such cases, the method is applied twice. In the first step, determination of unknown coupling constants is performed (as will be shown in the next section). Then, complete deconvolution of the spectrum is obtained using the above strategy.

APPLICATION TO DETERMINATION OF COUPLING CONSTANTS

The *N*-channel MaxEnt method can be used to process spectra with unknown *J* values or even spectra of unknown molecules. Indeed, the spectroscopist always knows at least one component common to all c_k convolution functions, which depends only on the experiment type. For example, all peaks in a COSY spectrum arise from an active coupling component. Then, all c_k functions can be expressed as

$$c_k(t) = a(J_k,t) \times c'_k(t) \tag{23}$$

with

$$a(J_k,t) = \sin(\pi J_k t) \tag{24}$$

where $c'_k(t)$ contains passive coupling components, if ever.

It is possible to perform simultaneous deconvolution of all the active $a(J_k,t)$ modulations using *N* channels. Since these modulations differ not by nature but only by the values of their associated coupling constants J_k, each channel can be viewed as bearing the J_k value. Since all possible values J_k cannot be continuously tested, they are chosen in a given interval $[J_1,J_2]$ expected to be relevent

$$J_k = J_1 + (k-1) \times \Delta J \tag{25}$$

with

$$\Delta J = (J_2 - J_1)/(N - 1) \tag{26}$$

When convergence is reached, peaks with an active coupling constant close to a given J_k present significant intensities only in channel k.

This, together with deconvolution of all active modulations, provides a means to determine unknown coupling constants: automatic peak picking and integration in the N channels allows one to plot integrals of the deconvoluted peaks as a function of J_k. Spline interpolation between the J_k values is performed, giving an estimate of the coupling constants by the maxima positions. This is performed by a fully automated process in the GIFA program.

This approach is examplified on the 2D DQF-COSY spectrum of tryptophan, although the method also applies to 1D spectra. The fact that the actual values were accessible from the 1D spectrum was convenient to validate the approach. Diagonal peaks of protons 4 and 7 and cross peaks of the same protons (in the lower left half of the 2D map) were studied. Diagonal peaks of these two protons present only active coupling

$$c(t) = \sin(\pi J t_1) \times \sin(\pi J t_2) \tag{27}$$

while their cross peaks present active and passive couplings

$$c(t) = \sin(\pi J t_1) \times \sin(\pi J t_2) \times \cos(\pi J t_2) \tag{28}$$

For protons 4 and 7, five channels were defined. All channels contained the same type of modulation $a(J_k,t_1,t_2)$: a sine function in both dimensions. However, a different value of the coupling constant J_k was used in each channel

$$a(J_k,t_1,t_2) = \sin(\pi J_k t_1) \times \sin(\pi J_k t_2)$$

$$J_k = J_1 + (k - 1) \times \Delta J$$

$$[J_1,J_2] = [4,12]$$

$$\Delta J = 2 \text{ Hz} \tag{29}$$

Similarly, in the case of protons 5 and 6, five channels were defined

$$a(J_k,t_1,t_2) = \sin(\pi J_k t_1) \times \sin(\pi J_k t_2)$$

$$J_k = J_1 + (k - 1) \times \Delta J$$

$$[J_1,J_2] = [6,10]$$

$$\Delta J = 1 \text{ Hz} \tag{30}$$

The choice of different channels in eqs 29 and 30 was made to test the consistence of the method, when used under different conditions. The interpolation curves are shown in Figure 7a,b. The maxima lead to an estimated coupling constant varying from 8.1 to 8.4 Hz. These values are in good agreement with the 8.2 Hz value, as obtained from the 1D spectrum (see the above section). These results show that the method gives satisfying results, even when applied in different conditions, on various multiplets presenting various fine structures. It is interesting to note that the estimated coupling constants differ from 8.2 Hz by less than the digital resolution of the DQF-COSY map (1.5 Hz/pt in dimension 1 and 3 Hz/pt in dimension 2). In this example, all values of the coupling constants were equal, but the method would apply similarly with different values.

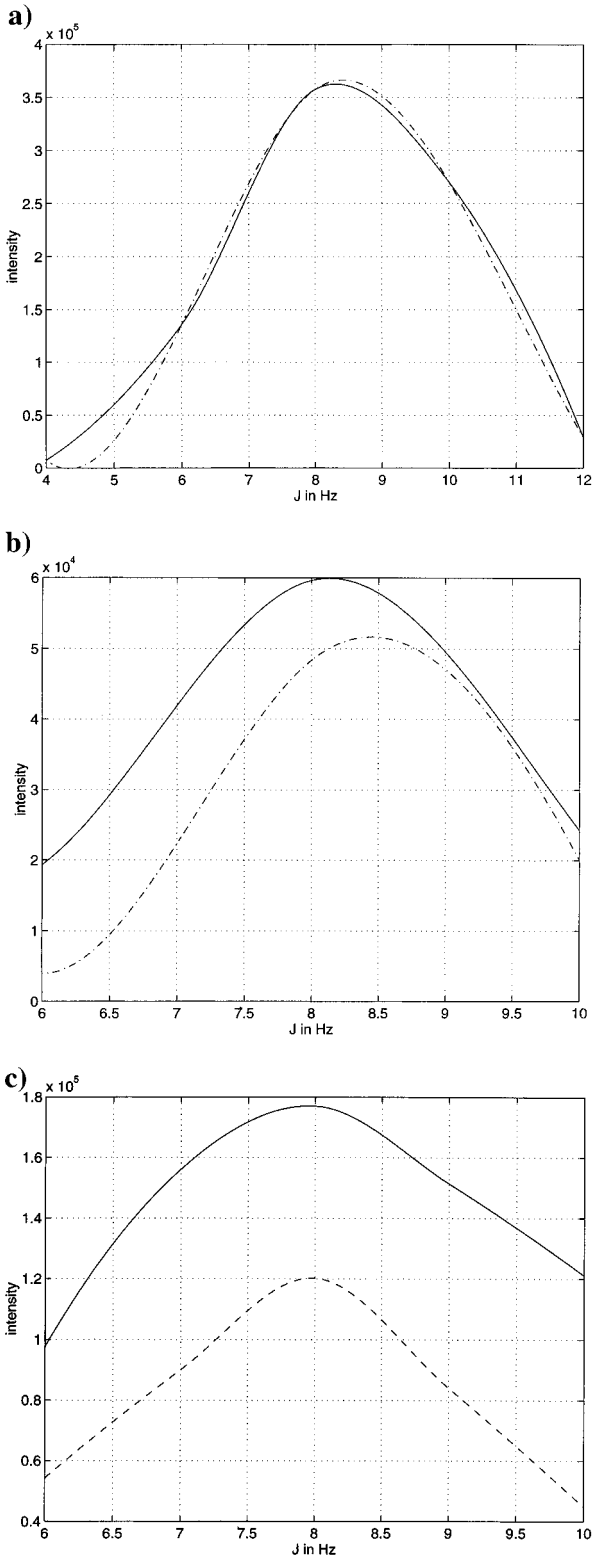

Figure 7. (a) Spline interpolation of the integral of the deconvoluted diagonal peaks of protons 4 (solid line) and 7 (dashed dotted line), as a function of J_k. The positions of the two maxima correspond to 8.4 Hz (proton 4) and 8.3 Hz (proton 7). (b) Spline interpolation of the integral of the deconvoluted cross peaks of protons 4 (solid line) and 7 (dashed dotted line), as a function of J_k. The positions of the two maxima correspond to 8.4 Hz (proton 4) and 8.1 Hz (proton 7). (c) Spline interpolation of the integral of the remaining in-phase components of the deconvoluted diagonal peaks of protons 6 (solid line) and 5 (broken line), as a function of J_k. The positions of the two maxima correspond to 8.0 Hz.

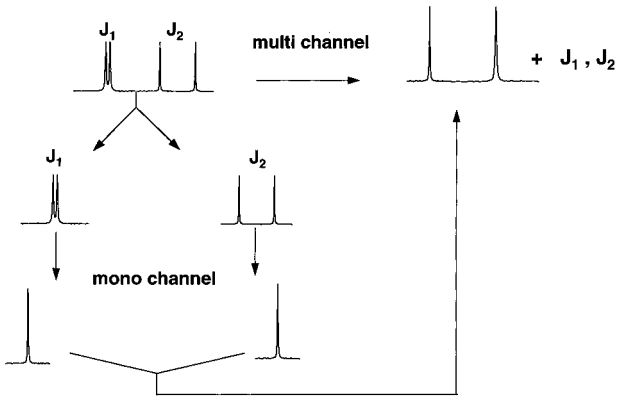

Figure 8. In *N*-channel methods, all lines are simultaneously processed. In monochannel methods, multiplets have to be previously extracted before being processed separately.

N-channel deconvolution of all active modulations was obtained simultaneously to all active *J* coupling determination. In the resulting spectrum, passive couplings remained on the multiplets corresponding to protons 5 and 6. Nevertheless, the active coupling coupling constants can still be determined, by plotting the integral of the remaining in-phase components as a function of the active coupling constant. Such examples are shown in Figure 7c. A coupling constant of 8.0 Hz is found for the two diagonal peaks of protons 5 and 6. This value is also in agreement with those obtained for protons 4 and 7, considering the digital resolution of the 2D map. The remaining passive *J* values could also be determined, using the same strategy.

DISCUSSION

It is important to stress that monochannel methods cannot achieve deconvolution of a complete spectrum in a single step. They first imply extraction of each multiplet from the original spectrum. Deconvolution is performed separately, as illustrated in Figure 8. Indeed, monochannel methods cannot achieve deconvolution of a given multiplet, in the presence of other multiplets of different fine structures. In monochannel methods, the degree of convergence is evaluated by global criteria on the whole data. Thus, signals arising from multiplets of unrelevent modulation are taken into account. Therefore, when convergence is apparently reached not only are strong artefacts present on those multiplets but also correct deconvolution is not observed on the multiplet of interest. As a consequence, it is not possible to process different channels sequentially or on parallel computers using monochannel methods. Similarly, monochannel methods involving a systematic variation of the modulation, using a distance criteria such as χ^2 to check for matches, will only be suitable if a single modulation is present in the spectrum. Such approaches cannot be understood as *N*-channel methods.

The above examples prove that the MaxEnt method can be generalized in NMR to *N*-channel deconvolution. It is important to stress that, in the case of 2D NMR, a genuine 2D algorithm is used, rather than a 1D algorithm applied on rows and columns. Therefore, its use in 2D NMR is simple and automatic. However, in the case of large data sets, the spectrum needs to be cut in boxes (depending on *N*, the number of channels needed), because the arrays used in the program have a limited size

$$N \times size(data) \leq 256^3$$

As expected, notable improvement in resolution and S/N is observed in the reconstructed spectra.

The approach presented in this paper can be used whether or not the complete *J* pattern is known. In the latter case not only deconvolution of the spectrum is achieved but also the unknown coupling constants are determined. This is very interesting when the coupling constants are not accessible because of overlaping peaks or complex *J* patterns: in the deconvoluted spectrum, a better resolution is recovered.

The calculation time is insensitive to the number of multiplets or to their complexity and their variability in modulation. The numbers of explored channels and of data points are the only parameters that have to be fixed, and that will affect the calculation time. In all cases, the number of iterations necessary for convergence was small, in the order of 10−20 iterations.

As in other inverse reconstruction methods,[20,21] MaxEnt also enables partial deconvolution of the line width.[14] Hence, partial line width deconvolution has been systematically combined to fine structure deconvolution, by adding an exponential damping term to the convolution expression function

$$c'(t) = c(t) \times \exp(-t/\tau)$$

Then, NMR lines undergo line width reduction of $1/\pi\tau$. This characteristic also contributes to S/N enhancement. Indeed, a damping envelope is present on all signals. Thus, a better convergence is usually observed (smaller values of χ^2) when a similar damping envelope is also present in the deconvolution function.

In conclusion, the method presented here separates chemical shift and line shape information (i.e., *J* coupling information), which can simplify "everyday" spectral analysis. This *N*-channel MaxEnt approach is implemented in the Gifa software, a complete NMR data processing software and available upon request.[14−22] Gifa is written in Fortran and C, and it is available for most UNIX platforms. Calculation times depend on the data sizes and the number of channels. For a 256 × 256 points experiment, and five channels, convergence is reached approximately in 10 min, on an Indy Silicon Graphics workstation. In the Gifa program, the method described here can be called just as any other conventional tool (base-line correction, phasing, etc....), appearing to the nonspecialist user as an option of the program. It has been designed to be fully automated so that no methodological difficulty is encountered by the user.

ACKNOWLEDGMENT

We would like to thank Dr. Michel Robin and Dr. Daniel Abergel for valuable discussions, reading the manuscript, and for their constant support.

REFERENCES AND NOTES

(1) Eberstadt, M.; Gemmecker, G.; Mierke, D.; Kessler, H. Scalar coupling constants—Their application for the elucidation of structure. *Angew. Chem., Int. Ed. Engl.* **1995**, *34*, 1671−1695.
(2) Aue, W. P.; Karhan, J.; Ernst, R. R.; Homonuclear broad band decoupling and two-dimensional J-resolved NMR spectroscopy. *J. Chem. Phys.* **1976**, *64*, 4226−4228.
(3) Novic, M.; Eggenberger, U.; Bodenhausen, G.; Similarities between self-convolution and symmetry mapping of multiplets in two-dimensional NMR spectra. *J. Magn. Reson.* **1988**, *77*, 394−400.
(4) Hubber, P.; Bodenhausen, G. Accurate determination of scalar couplings by convolution of complementary two dimensional multiplets. *J. Magn. Reson., Ser. A* **1993**, *103*, 118−121.

(5) Le Parco, J. M.; McIntyre, L.; Freeman, R. Accurate coupling constants from two dimensional correlation spectra by "J Deconvolution". *J. Magn. Reson.* **1992**, *97*, 553−567.
(6) McIntyre, L.; Freeman, R. Accurate measurement of coupling constants by J doubling. *J. Magn. Reson. Series A* **1994**, *111*, 425−431.
(7) Delsuc, M. A.; Levy, G. C. The application of maximum entropy processing to the deconvolution of coupling patterns in NMR. *J. Magn. Reson.* **1988**, *76*, 306−315.
(8) Jones, J. A.; Grainger, D. S.; Hore, P. J.; Daniell, G. J. Analysis of COSY cross peaks by deconvolution of the active splittings. *J. Magn. Reson. Ser. A* **1993**, *101*, 162−169.
(9) Meier, B. U.; Madi, Z. L.; Ernst, R. R. Computer analysis of nuclear spin systems based on local symmetry in 2D spectra. *J. Magn. Reson.* **1987**, *74*, 565−573.
(10) Woodley, M.; Freeman, R. "Decoupled" proton NMR spectra. *J. Magn. Reson. Ser. A* **1994**, *109*, 103−112.
(11) Woodley, M.; Freeman, R. A new scheme for two-dimensional NMR shift correlation. *J. Am. Chem. Soc.* **1995**, *117*, 6150−6151.
(12) Sibisi, S. Two-dimensional reconstructions from one-dimensional data by maximum entropy. *Nature* **1985**, *301*, 134−136.
(13) Hodgkinson, P.; Mott, H. R.; Driscoll, P. C.; Jones, J. A.; Hore, P. J. Application of maximum entropy methods to three-dimensional NMR spectroscopy. *J. Magn. Reson., Ser. B* **1993**, *101*, 218−222.
(14) Delsuc, M. A.; Robin, M.; Van Heijenoort, C.; Reisdorf, C.; Guittet, E.; Lallemand, J. Y. *Aspects of the study of biological Macromolecules by Nuclear Magnetic Resonance Spectroscopy*; Hoch, J. C., Ed.; Plenum Press: New York, 1991.
(15) Shore, J. E.; Johnson, R. W. Axiomatic derivation of the principle of maximum entropy and the principle of minimum cros- entropy. *IEEE Trans. Inform. Theor.* **1980**, *IT-26*, 26.
(16) Lieu, R.; Hicks, R. B.; Bland, C. J. Maximum entropy in data analysis with error carrying constraints. *J. Phys. Math. Gen.* **1987**, *20*, 2397−2388.
(17) Delsuc, M. A. *Maximum Entropy and Bayesian Methods, Cambridge, England, 1988*; Skilling, J., Ed.; Kluver Academic Publishers: Dordrecht (The Netherlands), 1989.
(18) Gull, S. F.; Daniell, G. J. Image reconstruction from incomplete and noisy data. *Nature* **1978**, *272*, 686−690.
(19) Stoven, V.; Mikou, A.; Piveteau, D.; Guittet, E.; Lallemand, J. Y. PARIS, a program for automatic recognition and integration of 2D NMR signals. *J. Magn. Reson.* **1989**, *81*, 163−168.
(20) Barkhuijsen, H.; de Beer, R.; Bovee, W.; van Ormondt, D.; Retrieval of frequencies, amplitudes, damping factors and phases from time-domain signals using a linear least-squares procedure. *J. Magn. Reson.* **1985**, *61*, 465−481.
(21) van der Veen, J.; de Beer, R.; Luyten, P.; van Ormondt, D. Accurate quantification of *in vivo* ^{31}P NMR signals using the variable projection method and prior knowledge. *Magn. Reson. Medicine* **1988**, *6*, 92−98.
(22) Pons, J. L.; Malliavin, T. E.; Delsuc, M. A.; Gifa V4: a complete package for NMR data-set processing. Submitted to *J. Bio. NMR.*

CI960321N